The Space Congress® Proceedings | 1964 (1st) - Where Are We Going In Space?

Apr 1st, 8:00 AM

Microwave, Over wafer, Multipath Propagation Tests at the Mistram Eleuthera Site

E. W. HeInzerling
Radio Guidance Operation, General Electric Company, Syracuse, New York

Follow this and additional works at: https://commons.erau.edu/space-congress-proceedings

Scholarly Commons Citation

HeInzerling, E. W., "Microwave, Over wafer, Multipath Propagation Tests at the Mistram Eleuthera Site" (1964). *The Space Congress® Proceedings*. 2.
https://commons.erau.edu/space-congress-proceedings/proceedings-1964-1st/session-2d/2

This Event is brought to you for free and open access by the Conferences at Scholarly Commons. It has been accepted for inclusion in The Space Congress® Proceedings by an authorized administrator of Scholarly Commons. For more information, please contact commons@erau.edu.

EMBRY-RIDDLE Aeronautical University
SCHOLARLY COMMONS

MICROWAVE OVER-WATER MULTIPATH PROPAGATION TEST AT THE MISTRAM ELEUTHERA SITE

E. W. Heinzerling
Radio Guidance Operation
General Electric Company
Syracuse, New York

Summary

A multipath propagation test using the sweep frequency technique was performed over the 28-mile over-water path between Mistram Central Station and Powell Point at Eleuthera, B.W.I. during November of 1963. Large ocean reflected signals were noted. Test results show path length differences between the direct and reflected signal up to six times larger than the theoretically computed values taking into account earth curvature and 4/3 earth type of refraction corrections. The relative magnitude of the reflected signal with respect to the direct signal varied between 0.3 and 0.96.

Poor correlation between multipath phenomena and measured weather data was noted.

Application of the results of this study to improving the reliability of a frequency diversity communication link are discussed.

Introduction

Since the installation of the Mistram II Missile Trajectory Measuring System at Eleuthera in the British West Indies there has been considerable interest in understanding the microwave propagation characteristics of an over-water path. It was felt that this understanding would permit the optimum design of electronic equipment which was to be used in this environment.

During the fall of 1962, the National Bureau of Standards conducted a propagation test between the Mistram Central Station and Powell Point, a distance of about 28 miles.[12] This test measured the amplitude and phase variations experienced over this link. The experimental data was reduced to obtain the statistical properties of the amplitude and phase variations. A strong reflected signal from the ocean surface was suspected as being the cause of the violent amplitude and phase variations noted. In order to investigate this possibility, barge mounted screens were positioned perpendicular to the direction of propagation at the calculated point of specular reflection. It was reasoned that if ocean reflections were the cause of the amplitude and phase variations, then these specially designed screens would block the reflected signal and reduce the amplitude of the fluctuations. Little improvement was noted using this technique.

In the meantime, the General Electric Company developed an instrument for measuring multipath propagation characteristics. Utilizing the latest developments in broadband microwave technology, the instrument was capable of resolving extremely small propagation path differences between two signals; path length differences of 0.1 feet or more could be measured. In the fall of 1963 this equipment was installed to investigate the same propagation path previously measured by the National Bureau of Standards.

The purpose of this paper is to:

1. describe the tests that were performed

2. present the experimental results obtained

3. to demonstrate one use of these results in the optimization of a typical frequency diversity communication link.

Multipath Characteristics

A radio communication link is said to be experiencing multipath transmission if the received signal may be derived from the vector addition of two or more distinct signals, each traveling over its separate path. The general multipath situation that will be discussed, in which the propagating medium produces three distinct paths, is illustrated in Figure 1. The shortest path is arbitrarily labeled the direct signal; it has a relative magnitude of 1.0 and an effective propagation distance, R.

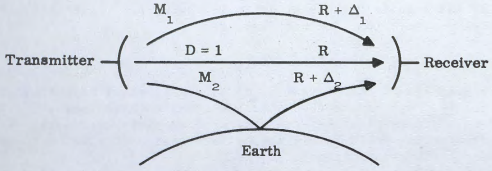

Figure 1. Multipath Transmission with Three Distinct Paths

The upper multipath has a relative magnitude of M_1 and an effective propagation path of $R + \Delta_1$. This multipath is caused by atmospheric anomalies.

The lower multipath has a relative magnitude of M_2 and an effective propagation distance of $R+\Delta_2$. This multipath is caused by reflection from the earth's surface. A 180-degree phase reversal occurs upon reflection at the grazing angles of incidence to be considered. (This is true for both horizontal and vertical polarization.) The effect of the additional path length, Δ, in the propagation path of the multipath signal is to cause an additional phase delay with respect to the direct signal. This phase delay may be expressed as

$$\theta = \frac{2\pi f \Delta}{c} \text{ radians,} \qquad (1)$$

where f is the frequency, Δ is the path length difference, and c is the velocity of propagation. Using the example shown in Figure 1, the received signal can be represented as the vector addition of three vectors as shown in Figure 2.

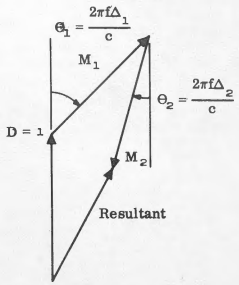

Figure 2. Vector Addition of Three Vectors

The resultant vector is completely determined from a knowledge of the relative magnitude and additional path lengths of the multipath vectors.

Principle of Measurements

Several techniques may be used to measure the presence of multipath propagation. (See References 1 through 6.) Among the more important techniques are the following:

a. Narrow Pulse Transmission

Multipath propagation would be present if two or more pulses are received for each transmitted pulse.

b. Angle of Arrival Measurements

A narrow-beam antenna is rotated in the vertical plane (similar to the rotation of a height-finding radar). Multipath transmission is present if appreciable energy is received at two or more elevation angles.

c. Sweep Frequency Technique

The transmitter is swept in frequency. In the presence of multipath transmission, the received amplitude versus frequency display will have a characteristic multipath signature that is attributable to the rotation of the multipath vector or vectors, with respect to the direct path, as the frequency changes.

d. Interference Pattern Measurement

A small sampling antenna is used to measure the vertical interference pattern produced by the vector addition of the direct and multipath vectors.

If very small rapid path length differences are to be detected, the sweep frequency technique is the most promising. With the recent development of the backward wave oscillator and the traveling wave tube, it is possible to sweep over a band of about 40 percent of the center frequency, which--if it is centered in the X-band region--would allow path length differences of 0.1 foot and larger to be measured.

The sweep frequency technique is illustrated in Figure 3 for the case of reflections from the ocean surface. For simplicity, only one multipath signal will be considered.

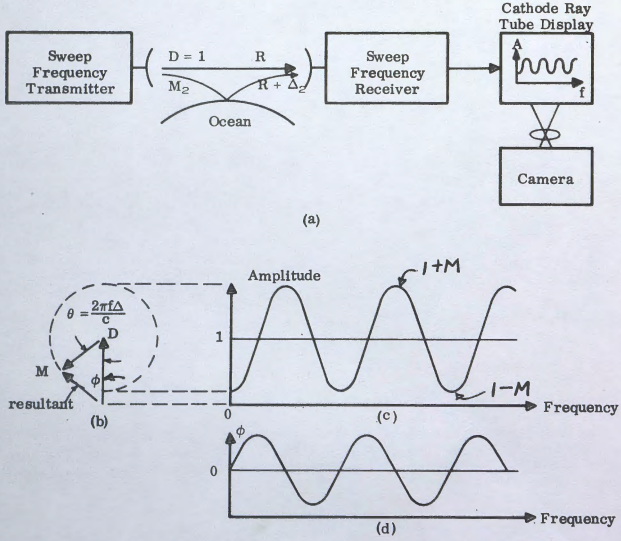

Figure 3 Sweep Frequency Technique

The output of the transmitter is propagated over the multipath environment that is to be measured. The magnitude of the vector resultant of the direct and and multipath signal is received and displayed on the oscilloscope as a function of frequency. From the vector diagram (see Figure 3(b)) it can be seen that as the frequency is increased, the multipath vector will rotate in the clockwise direction through an angle which is directly proportional to frequency.

The corresponding amplitude of the resultant vector is shown in Figure 3(c).

In addition to the amplitude variation, the multipath vector is capable of producing a phase variation as a function of frequency, which is shown in Figure 3(d). The relative magnitude of the multipath signal, M, with respect to the direct signal, D, may be easily calculated from the ratio of the maximum to minimum signal level since the maximum is 1+M and the minimum is 1 − M. The additional path length, Δ, may be calculated from the frequency difference between successive nulls. The nulls occur at frequencies for which

$$2n\pi = \frac{2\pi f \Delta}{c} \text{ radians for } n = 0, 1, 2, 3 \qquad (2)$$

so that the path length difference may be expressed as

$$\Delta = \frac{c}{f_\delta} \qquad (3)$$

where f_δ is the frequency between successive nulls.

In the event that two or more multipath signals are present, the complex display of resultant amplitude versus frequency will, in general, require reduction into its individual multipath components by means of a simulator.

Equipment

Transmitter

A simplified block diagram of the transmitter is shown in Figure 4. The transmitter consists of a backward wave oscillator that linearly sweeps between 6.5 kilomegacycles and 11.0 kilomegacycles at a 10-cycle per second rate. The RF output is amplified by a wideband traveling wave tube amplifier and delivered to the antenna through the broadband sampler.

The sampler produces a d-c voltage that is proportional to the RF signal. This voltage is compared to a voltage reference that corresponds to the desired RF output. The difference voltage is amplified and then used to vary the backward wave oscillator output in such a way as to maintain the sampler voltage equal to the reference voltage. This feedback arrangement keeps the output signal reasonably constant in spite of the violent power variation that would normally be expected when a backward wave oscillator and traveling wave tube are used over such a wide bandwidth.

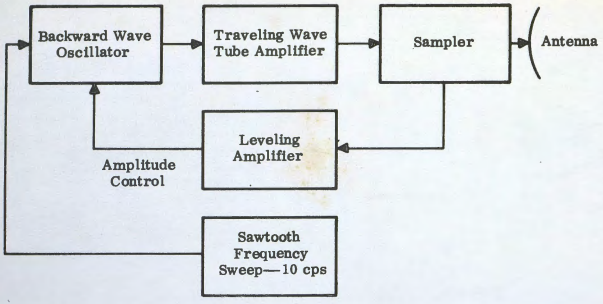

Figure 4 Transmitter, Simplified Block Diagram

Receiver

A simplified block diagram of the receiver is shown in Figure 5. The associated display and recording equipment is shown in simplified block diagram form in Figure 6.

The sweep frequency receiver is designed to follow in frequency the linear frequency sweep of the associated transmitter. It consists essentially of a frequency-lock loop with a sweep assist channel in order to permit the large frequency deviation of the incoming signal to be followed.

The received signal is mixed with the local oscillator in the special broadband mixer located directly behind the tower-mounted receiving antenna. The resultant 30-megacycle intermediate frequency is amplified in a 60-db amplifier, which is also tower-mounted. The amplified signal is transmitted down the tower to the step attenuator, where various fixed attenuations can be switched in the signal path to bring the absolute received level to an acceptable value. Two additional stages of fixed amplification are added before detection. Two detectors are available. One is a linear detector which produces a low-frequency signal output that is linearly proportional to the intermediate frequency signal. The other is a logarithmic detector which has the capability of expanding the lower signal levels. All the data analyzed in this report was obtained with the linear detector.

A frequency-lock loop with sweep assist is used to obtain accurate tracking of the local oscillator.

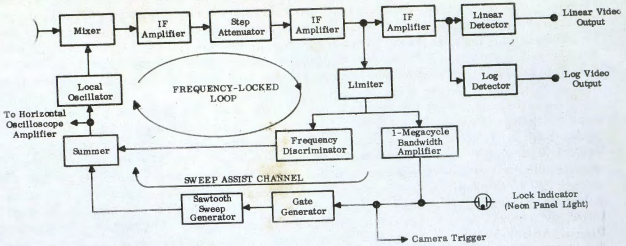

Figure 5 Sweep Frequency Receiver, Simplified Block Diagram

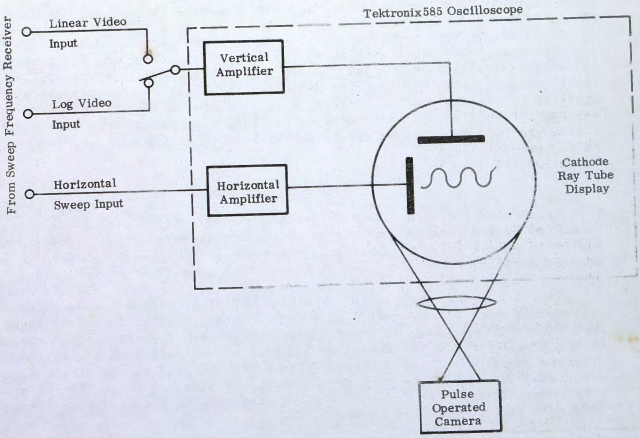

Figure 6 Display and Recording Equipment, Simplified Block Diagram

A portion of the IF signal is hard-limited in order to obtain a signal output for which the amplitude is constant irrespective of the level of the input signal. One output of the limiter is applied to the frequency discriminator where a voltage proportional to the instantaneous frequency deviation from 30 megacycles is produced. This voltage passes through the summer and is applied to the backward wave local oscillator in order to control the frequency of this oscillator with respect to the received signal so that the required 30-megacycle IF is produced.

In order to reduce the gain requirements of the frequency-locked loop, a sweep assist channel is employed to produce the sawtooth voltage required by the local oscillator. This is implemented by using the second output of the limiter. Before the start of the receiver sweep, the local oscillator is preset to oscillate at the low-frequency end of the frequency spectrum. When the transmitter sweep is 30 megacycles below the frequency of the preset receiver local oscillator, a narrow pulse is produced at the output of the 1-megacycle bandwidth amplifier. This pulse triggers the gate generator, which in turn initiates the sawtooth. The sawtooth sweep is summed with the output of the frequency discriminator and applied to the local oscillator in order to produce the predominant portion of the frequency sweep voltage. The frequency-locked loop signal then corresponds to the error between the transmitter and receiver sawtooths.

In addition to the two video output signals, the receiver provides a sawtooth signal that is proportional to frequency for horizontal deflection of the oscilloscope display and a camera trigger for synchronizing the shutter and film pull-down of the pulse-operated camera.

The simplified block diagram of the display and recording equipment is illustrated in Figure 6. A Tektronix 585 oscilloscope is used to produce the oscilloscope display. Either the linear or the logarithmic video signal is employed to produce the vertical deflection, while the local oscillator sweep voltage is used for the horizontal deflection. The cathode ray tube display is then a plot of the received signal-versus-frequency with a repetition rate of 10 sweeps per second.

Experimental Results

Measurements over the Central Station - Powell Point propagation path were conducted during November and the early part of December 1963. Typical resultant amplitude versus frequency photographs are shown in Figures 7 through 10 which were selected to illustrate some of the extreme conditions encountered.

During a normal test, a new resultant amplitude versus frequency photograph was exposed every 1.6 seconds. In order to conserve film, bursts of about 10 frames were taken every 15 minutes. One typical photograph from each burst was reduced to obtain a value of the additional path length of the multipath signal, Δ, and the relative magnitude of the multipath signal with respect to the direct signal. The results of this reduction on a typical test are shown in Figure 11, in which the path length difference, Δ, and relative magnitude of the multipath signal are displayed as a function of time.

The dominant multipath signal was produced by ocean reflection. The path length difference varies between 0.09 and 0.4 foot, and the relative magnitude varied between 0.3 and 0.96. The larger values of relative magnitude are difficult to read accurately and it is therefore probable that values of relative magnitude larger than 0.96 were experienced from time to time. Theoretically, the reflected

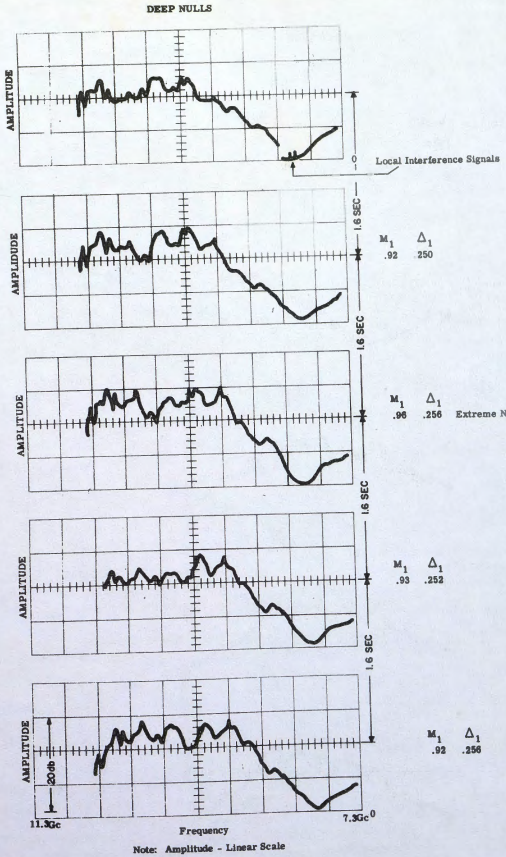

Figure 7 - Experimental Results

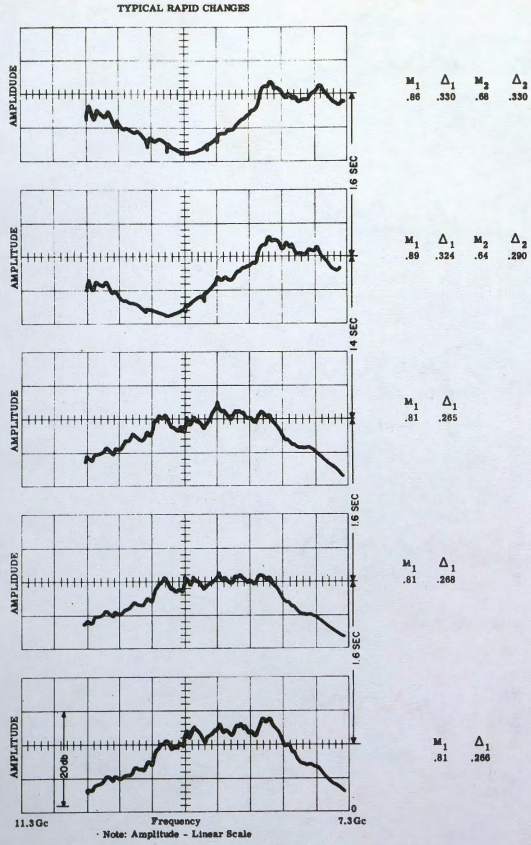

Figure 8 - Experimental Results

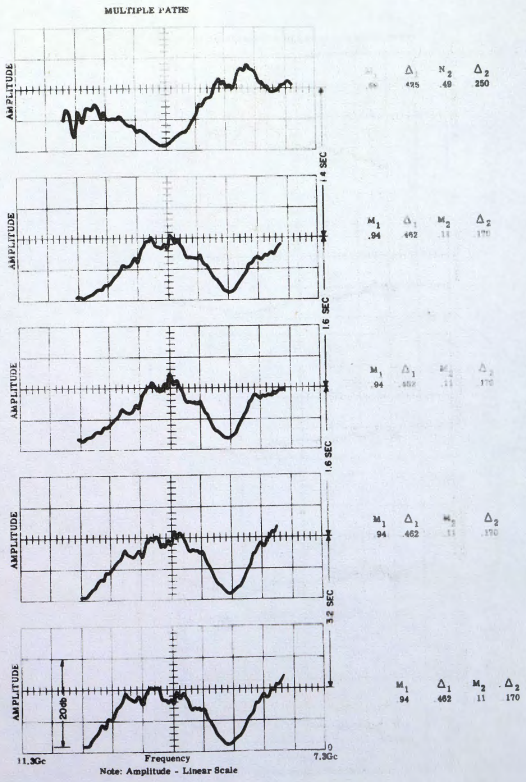

Figure 9 Experimental Results

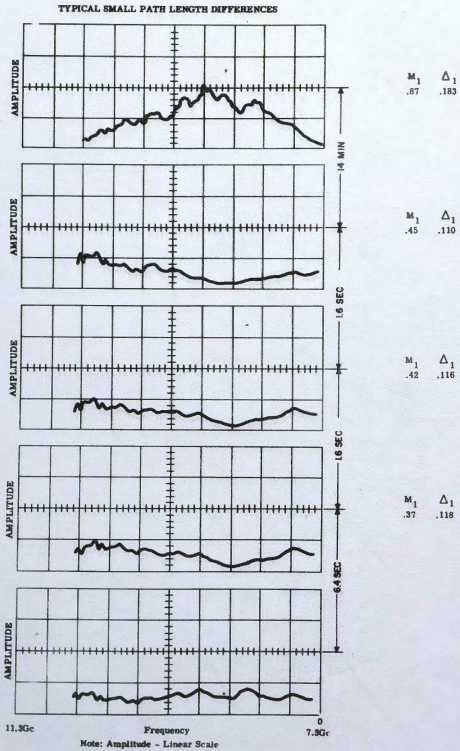

Figure 10 - Experimental Results

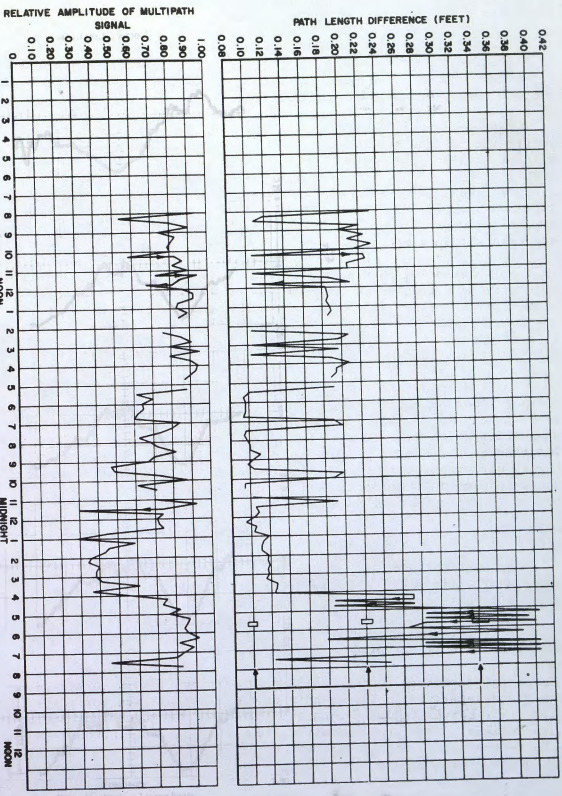

Figure 11

- Typical Path Length Difference, Δ , and Relative Amplitude versus Time

signal should be reduced from unity by the value of the divergence factor which is calculated in Reference 15, Appendix A to be about 0.52. This average magnitude is in approximate agreement with theoretical calculations. The wide variations in the relative magnitude must be produced by meteorological and ocean fluctuations whose exact origins are presently unknown.

The measured value of path length difference was usually (up to six times) much greater than the theoretically calculated value of 0.06 derived in Reference 15, Appendix B and C, by accounting for the earth curvature and ray bending using the 4/3 earth approximation.

These large values are of a magnitude which could be attributed to differential refraction between the two paths (for which no correction was made) and/or due to changes in the apparent center of multipath reflection due to sea conditions.

At times, large values of path length difference occurred simultaneously with rapid variations in path length difference. This is well illustrated in Figure 11 between 5:00 and 7:00 A.M., where large changes in path length differences often occurred within a matter of seconds.

An interesting phenomena occurred on the afternoon of 6 November 1963 when thunderstorm activity was observed in the vicinity of the propagation path. At this time, the absolute signal level increased by about 20 db at all frequencies and no multipath transmission was observed. After several hours, the propagation path returned to its normal condition. This phenomenon is characteristic of ducting (see Reference 10).

A large amount of weather data was accumulated during the multipath tests in the hope that multipath results could be correlated with some meteorological characteristic. Part of the recorded weather data was reduced to obtain some derived quantities which were also used in the correlation. All the available weather data was then plotted as a function of time and visually correlated with plots of path length difference and relative magnitude of the reflected signal. Unfortunately, not enough correlation was noted between the quantities to be of any help in predicting poor propagation conditions.

Application

The previous section illustrated the typical multipath parameter variations of an over water path. In this section, it would be of interest to apply these results to optimize a frequency diversity communication link.

A typical frequency diversity communication link operating in a multipath environment is illustrated in Figure 12.

The information to be transmitted over the link is modulated on two carriers which are separated in frequency. At the terminal each carrier is received by a separate receiver, and the outputs of the two receivers are combined to yield one output signal. The combination process may be produced by a simple switch which selects the output of the receiver with the strongest input signal, or a more elaborate combination process may be used.

For illustrative purposes in this paper let us consider that a simple switch is used to select the receiver with larger input signal.

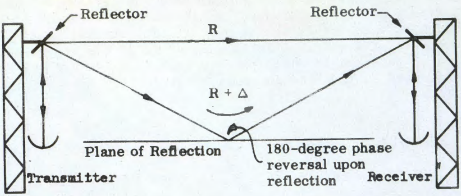

Figure 12 - Typical Frequency Diversity Communication Link

In a frequency diversity communication link, it is reasoned that the propagation conditions experienced by the two separate carriers frequencies are sufficiently different so that the probability of both carriers simultaneously experiencing deep fading conditions is extremely small.

For carrier frequencies in the X-band region, a frequency separation of between 2 and 4 percent would be typical. This corresponds to frequency separation of about 200 MC. In general, this degree of frequency separation is usually sufficient to produce uncorrelated noise at the receiver, when this noise is generated in the atmosphere. It would now be of interest to calculate the performance of our typical frequency diversity communication link in an ocean reflected multipath environment. As illustrated by the experimented data in Figure 7 through 11, the presence of the reflected signal causes severe fading at certain frequencies, the exact frequency being a function of the path length difference. A typical amplitude versus frequency spectrum is illustrated in Figure 13 below.

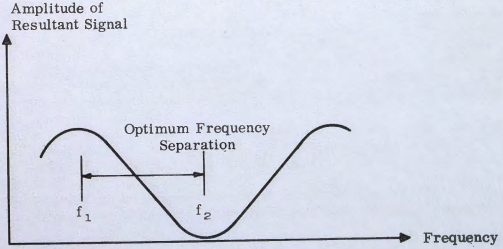

Figure 13 - Typical Amplitude versus Frequency Display

From this figure, it can be concluded that the optimum frequency diversity action will result if the two frequencies of the communication link are positioned in the spectrum so that one is at the peak of the received amplitude spectrum while the other is at a null. A horizontal shift of the amplitude spectrum curve may result in an exchange in which carrier frequency has the higher amplitude and is, therefore, used to complete the communication link but will not cause communication failure.

In proceeding, it would be beneficial to examine this rather obvious conclusion in more detail in order that quantitative results may be obtained.

As discussed in detail previously, the relative phase angle between the direct and multipath vector caused by the additional path length, Δ, of the reflected signal is given as:

$$\theta = \frac{360 f \Delta}{C} \text{ degrees}$$

where f is the operating frequency and C is the velocity of light. Because of the slight difference in carrier frequencies, the phase shift produced by multipath at each carrier frequency will be slightly different. In particular, let the phase shift produced at the higher frequency f_1 be θ_1 and that at the lower frequency, f_2 by θ_2. In addition, let the path length difference, Δ, be common for both frequencies. The vector diagram corresponding to the two received signals

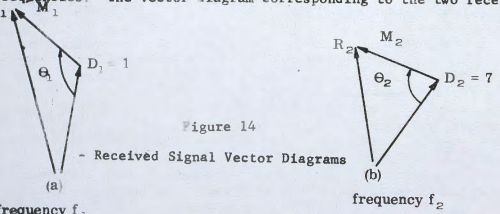

Figure 14 - Received Signal Vector Diagrams

are drawn in Figure 14. In the diagrams, the direct-signal vectors are each assumed to be of unity magnitude and the multipath vectors to have a relative magnitude of $M = M_1 = M_2$ with respect to the direct vector. Under the above conditions, it can be seen that the relative value of the resultant vector at each frequency is determined from a knowledge of θ_1, θ_2 and M. In order to simplify the comparison between the two resultant vectors, the two direct signal vectors may be superimposed which would produce the vector diagram of Figure 15.

As the path length difference, Δ, increases, both θ_1 and θ_2 will increase. Because of its higher frequency θ_1 will increase at a faster rate than θ_2 and the differential phase shift $\delta\theta$ will, therefore, also increase as a function of Δ

Each of the resultant vectors will undergo the typical amplitude pertubations as a function of path length difference illustrated in Figure 16.

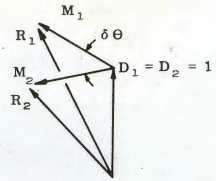

$$\Theta_1 = \frac{360\, f_1\, \Delta}{C}$$

$$\Theta_2 = \frac{360\, f_2\, \Delta}{C}$$

$$\delta\Theta = \frac{360\, \delta f\, \Delta}{C}$$

where

$$\delta f = f_1 - f_2$$

Figure 15 - Superposition of Received Signal Vectors

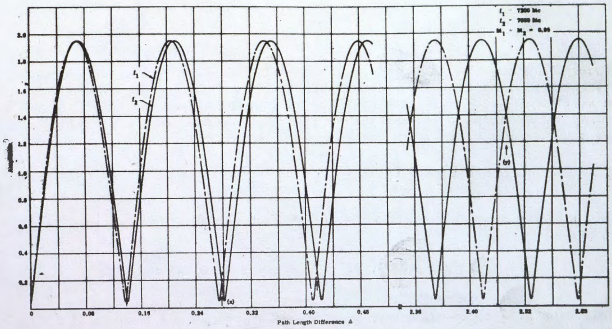

Figure 16 - Received Signal Amplitude versus Path Length Difference

In generating these curves, the direct signal vectors are each assumed to be of unity magnitude and the multipath vector to have a relative magnitude of M = .95 with respect to the direct vector. In addition, those values of path length difference, Δ, which cause the maximum simultaneous attenuation of both signals and which would represent the worst conditions under which the system would be required to operate are shown by the small arrows. It can also be seen that if the path lengths difference is large enough, an actual multipath path signal gain will occur. The vector diagram corresponding to those points of maximum simultaneous attenuation is illustrated in Figure 17.

The diagram of Figure 17a corresponds to point x of Figure 16, while Figure 17b corresponds to point (y).

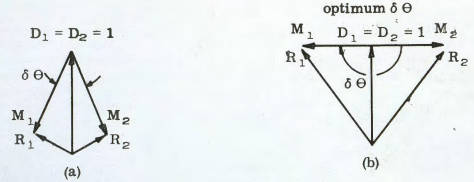

Figure 17 - Vector Diagrams for Poor (a) and Optimum (b) Frequency Diversity

Figure 17a shows the vector diagram for small values of $\delta\theta$ which can cause severe simultaneous attenuation while Figure 17b shows the vector diagram for an optimum system, in which multipath will actually produce a signal gain. From the vector diagram it can be seen that the parameter which describes the maximum possible simultaneous attenuation due to multipath is:

$$\delta\theta = \frac{360\ (\delta f)(\Delta)}{C}$$

and that the optimum system performance is achieved when $\delta\theta$ = 180 degrees. This occurs when:

$$(\delta f)\ (\Delta) = \frac{C}{2} = \frac{9.8 \times 10^8}{2} = 4.9 \times 10^8 \text{ ft/sec}$$

A typical curve of maximum simultaneous attenuation versus the product $(\delta f)\ (\Delta)$ is shown in Figure 18. A value of M = .95 was used in constructing this graph.

The peak in this curve illustrates the optimum value of the product of the differential frequency and the path length difference. In practice, the value of Δ may be expected to vary due to various meteorlogical conditions. In order to obtain a truly optimum system in a practical situation, the span of values of Δ actually experienced should be used in calculating the optimum frequency separation between channels.

It can be seen that the peak to the curve is rather broad so that the reasonable variations in Δ due to meteorlogical changes should produce only moderate degradation of system performance.

An optimum system, in the multipath sense, would have a differential frequency wavelength, $\lambda_{\delta f} = \frac{C}{\delta f}$, which is twice the path length difference. The path length difference would be calculated by taking the average of the maximum and minimum path length difference encountered.

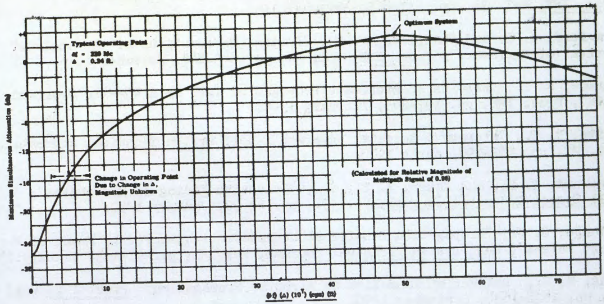

Figure 18 - Maximum Simultaneous Attenuation versus $\delta\phi$ (Δ)

Acknowledgement

The author wishes to acknowledge the outstanding efforts of Mr. J. J. Gaura who was in charge of the field testing phase at Eleuthera and Antenna Park, and of the reduction of experimental data; the assistance of Mr. G. Tucker in the testing phase at Eleuthera, Mr. A. LaMacchia in the reduction of the experimental data.

Special mention should be made of the support given to this project by Lt. John Cribbs, USAF, AMR, who clearly saw the need for a test of this nature and supported the effort through the many obstacles encountered.

The excellent cooperation given in the field testing portion of this program by both Pan American and RCA personnel is sincerely appreciated.

This project was sponsored jointly by the Air Force Mistram Project Office and the General Electric Company.

List of References

1. Sharpless, W. M., "Measurement of the Angles of Arrival of Microwave", Proc. IRE, Vol. 34, pp. 837-845, November 1946.

2. Crawford, A. B. and Sharpless, W. M., "Further Observations of the Angle of Arrival of Microwave", Proc. IRE, Vol. 34, pp. 845-848, November 1946.

3. Durkee, A. L., "Results of Microwave Propagation Test on a 40-Mile Overland Path", Proc. IRE, pp. 197-205, February 1948.

4. Friis, H. T., "Microwave Repeater Reserach", Bell System Technical Journal, Vol. 27, pp. 183-198, April 1948.

5. Crawford, A. B., and Jakes, W. C., Jr., "Selective Fading of Microwaves", Bell System Technical Journal, Vol. 31, pp. 68-90, January 1952.

6. Delange, O. e., "Propagation Studies at Microwave Frequencies by Means of Very Short Pulses", Bell System Technical Journal, Vol. 31, pp. 91-103, January 1952.

7. Wong, M. S., "Refraction Anomalies in Airborne Propagation, "Proc. IRE, Vol. 46, pp. 1628-1638, September 1958.

8. Heinzerling, E. W., An Analysis of the Anomalous Behavior of the General Electric Mod III Lateral Rate at Low Elevation Angles as a result of Multipath (Secret), General Electric Company Internal Report, 10 November 1961.

9. Reed and Russell, Ultra High-Frequency Propagation, Wiley, 1953

10. Katzm, Bauchman, and Binnian; "Three-and-Nine-Centimeter Propagation in Low Ocean Ducts". Proc. IRE, Vol. 35, pp. 801-905, September 1947.

11. LaGrone, A. H., and Tolbert, C. W., Reflection Studies of Millimeter and Centimeter Radio Waves for Gulf of Mexico Paths, Electrical Engineering Research Laboratory, The University of Texas, Report No. CM 753.

12. Janes, Kirkpatrick, Waters, Smith, Phase and Amplitude Diversity in Over-water Transmissions at Two Microwave Frequencies, National Bureau of Standards, Report No. 7656, 26 February 1963.

13. Reference Data for Radio Engineers, Fourth Edition, International Telephone and Telegraph Company, pp. 742-747.

14. Chu, J. H., and Heinzerling, E. W., Theoretical External Effects Error Analysis of the Downrange Precision Missile Trajectory Measurement System, General Electric Company TIS R63-R607, 1 November 1962.

15. Heinzerling, E. W., Eleuthera Multipath Test, General Electric Company, 1 Januaty 1964.